Hemodynamics in AVF over time: A protective role of vascular remodeling toward flow stabilization

Luca Soliveri[1] iD **, Michela Bozzetto[1]** iD **, Paolo Brambilla[2,3],
Anna Caroli[1] and Andrea Remuzzi[4]**

Abstract

The mechanisms underlying vascular stenosis formation in the arteriovenous fistula (AVF) for hemodialysis (HD) remain mostly unknown. Several computational fluid dynamics (CFD) studies have suggested a potential role for unsteady flow in inducing intimal hyperplasia and AVF stenosis, but the majority of these observations have been limited to a single time point after surgical creation. The aim of the present study was to investigate the relation between hemodynamic conditions and AVF vascular remodeling through a CFD longitudinal study. Non contrast-enhanced MR images and Doppler Ultrasound (US) examinations were acquired at 3 days, 40 days, 6 months, 1 year, and 1.5 years after surgery in a 72-year male referred for native radio-cephalic AVF. Three-dimensional AVF models were generated and high fidelity CFD simulations were performed using pimpleFoam, setting patient-specific boundary conditions derived from US. Morphological and hemodynamic changes over time were then analyzed. Analysis of vessel morphology and hemodynamics during follow-up showed that the AVF had a successful maturation process, characterized by a massive arterial and venous dilatation within the 6 months after surgery, a corresponding increase in blood flow volume and important flow instabilities. Between 6 months and 1 year, a stenosis developed in the juxta-anastomotic vein and caused AVF failure at 1.5 years. The development of stenosis was paralleled by the regularization of blood flow velocity pattern and consequent decrease in the near-wall disturbed flow metrics. These results suggest that development of intimal hyperplasia and vessel stenosis, triggered by unsteady flow, could be the result of vascular inward remodeling toward regularization of turbulent-like flow.

Keywords

Arteriovenous fistula, hemodialysis, hemodynamics, longitudinal study, vessel remodeling

Introduction

Native arteriovenous fistula (AVF) is the vascular access (VA) for hemodialysis (HD) that is associated with the best outcomes,[1] but a 40% primary failure rate is still reported at 1 year after surgery.[2,3] Moreover, additional interventions are often needed to favor AVF maturation and to maintain AVF patency.[4]

The main cause of AVF failure is the development of stenosis in the juxta-anastomotic vein (JAV) due to neointimal hyperplasia (NH),[5,6] which consists in a complex proinflammatory response causing cell activation, proliferation and migration of smooth muscle cells (SMCs) in the intima layer. Stenosis formation is a multifactorial process, as it is triggered by a combination of clinical, hemodynamic and systemic factors,[7] such as surgical injury, hemodynamic shear stresses, repeated

[1]Department of Biomedical Engineering, Istituto di Ricerche Farmacologiche Mario Negri IRCCS, Bergamo, Italy

[2]Diagnostic Radiology, Papa Giovanni XXIII Hospital, Bergamo, Italy

[3]School of Medicine, University of Milano-Bicocca, Milan, Italy

[4]Department of Management, Information and Production Engineering, University of Bergamo, Italy

Corresponding author:
Michela Bozzetto, Istituto di Ricerche Farmacologiche Mario Negri IRCCS, Via Camozzi 5, Ranica (BG), Lombardy 24020, Italy.
Email: michela.bozzetto@marionegri.it

cannulations for HD treatment and genetic predisposition to prothrombotic disorders.[8]

Focusing on hemodynamics, already in 1999 Sivanesan[9] highlighted that vascular stenosis consistently develops in recurrent areas of the JAV, suggesting that focal neointimal growth might be related to local hemodynamic conditions. In recent years, a growing body of evidence has reinforced the hypothesis that the altered local hemodynamics acting on the endothelial cells (ECs), resulting from the surgically created vessel shunt, stimulate both the initiation and evolution of AVF stenosis.[10,11] In idealized AVF models, Ene-Iordache et al.[12] found specific spot regions exposed to athero-prone shear stress and Browne et al.[13] documented high pressure fluctuations in the AVF vein.

Although the use of computational fluid dynamics (CFD) has provided fundamental insights into the pathophysiology of AVF stenosis,[14] these studies have not shown a definitive link between any metric and disease development yet and, despite the clinical relevance, the mechanisms responsible for stenosis development in AVFs are still poorly understood.[15] We have previously demonstrated, using high-fidelity patient-specific CFD simulations, that transitional flow, characterized by high-frequency velocity and pressure fluctuations, is present in the venous segment of the AVF.[16] This evidence suggested a role for transitional flow in vascular remodeling and stenosis development. However, our previous investigation as well as most of the work from other groups, focused on a single observation at a given time after AVF surgery, while the sequence of events that develop after AVF creation, during VA maturation and in the following period, has not been investigated so far. Thus, there is an urgent need of performing longitudinal analysis of AVF morphological and hemodynamic changes starting from AVF surgical creation and in the following time period, up to AVF failure.

Our group has recently developed a non-contrast-enhanced magnetic resonance imaging (MRI) protocol that provides high-resolution black-blood images within an acquisition that lasts only a few minutes, allowing non-invasive and accurate imaging of patient's AVF morphology over time.[17] This MRI protocol, coupled with high-fidelity CFD simulations in a complete MRI-to-CFD pipeline, was used to characterize AVF morphology and hemodynamics at three different timepoints within the first year after the creation of AVFs with the VasQ device or using conventional surgery, and was proved to be a promising method for longitudinal evaluations in AVFs.[18]

The goal of the present study was then to investigate, at multiple timepoints, an AVF which ultimately failed at 1.5 years after surgical creation due to stenosis. In particular, we aimed at investigating the relation between vascular remodeling and the evolution of hemodynamic conditions.

Methods

A 72-year male affected by End Stage Renal Disease was referred for primary distal radio-cephalic side-to-end AVF at the Unit of Nephrology and Dialysis of Papa Giovanni XXIII hospital (Bergamo, Italy). The subject was not affected by preexisting vascular pathologies and prothrombotic disorders and did not perform any specific pre-operative or post-operative hand exercise to favor the increase of the venous caliber. After successful AVF maturation, the patient started HD treatment 43 days after surgery, twice a week with buttonhole cannulation.

Non-contrast-enhanced MRI examination was performed at 3 days after AVF surgical creation and then repeated at 40 days, 6 months, 1 year, and 1.5 years after surgery. The patient authorized the use of his clinical and imaging data for research purposes and their publication. Image acquisitions were executed using a 1.5T scanner (GE, Optima 450w GEM) with a flexible 16-channel phased array medium coil and were cardiac gated using peripheral pulse gating. A three-plane scout sequence acquisition was performed to correctly localize the anastomosis, and then 3D fast spin echo T1-weighted imaging was acquired using CUBE sequence, covering an arm region of approximately 5 cm above and 3 cm below the anastomosis. All the specifications on the MRI protocol can be found in our previous publication.[17] The MRI acquisition was preceded by a Doppler US examination of the AVF to measure blood flow volumes in the proximal artery (PA) and distal artery (DA).

Starting from MRI acquisitions, 3D AVF surface digital models were generated and pre-processed using the Vascular Modeling Toolkit (VMTK).[19] Straight cylindrical extensions of five diameters in length were added at the model's extremities to achieve a fully developed flow inside the computational domain. Based on a mesh refinement study, meshes of approximately 1000 k cells were obtained for all AVF models using FoamyHexMesh of OpenFOAM suite. Two thin boundary layers were generated to capture the sharp velocity gradients close to the vessel wall.

PimpleFoam, a transient solver for incompressible flows based on the finite volume method set with second-order spatial and time integration schemes in OpenFoam suit, was used to perform CFD simulations. Patient-specific inflow boundary conditions derived from Doppler US examinations were imposed as volumetric flow waveforms at the PA and DA, while for the vein outflow a traction-free condition was prescribed. Blood was modeled as non-Newtonian fluid exploiting the Bird-Carreau rheological model and assuming a blood density of $1.05\,g/cm^3$, patient's measured hematocrit and a total serum protein value equal to $7\,g/dL$. The no-slip condition was set at the vessel walls, which were
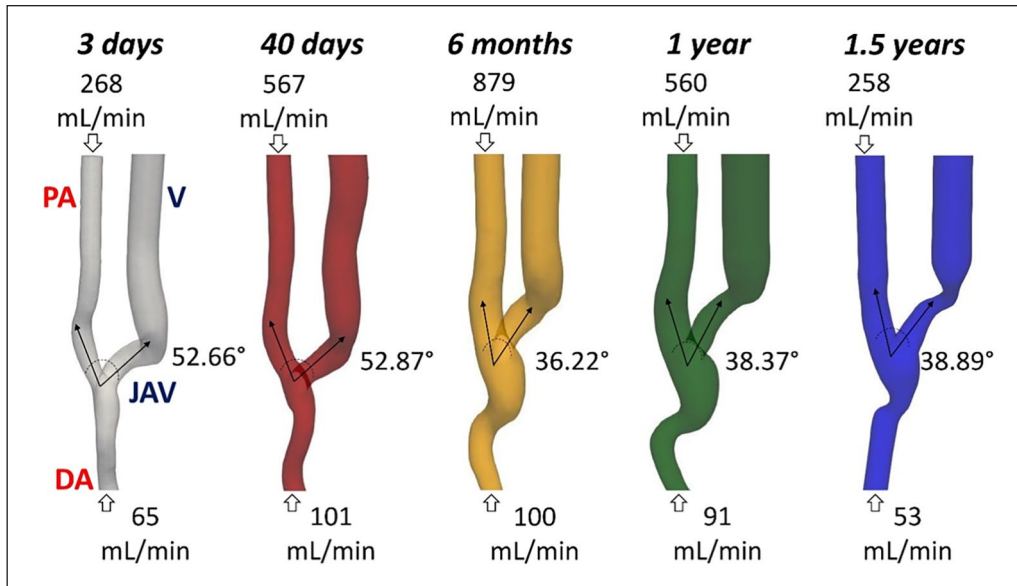
Figure 1. 3D geometrical AVF models and pertinent blood flow rates at five different timepoints after surgery.
AVF: arteriovenous fistula; PA: proximal artery; DA: distal artery; JAV: juxta-anastomotic vein; V: vein.
Black arrows indicate the main direction of the blood flow.

assumed to be rigid. Time discretization was automatically adjusted based on a maximum Courant–Friedrichs–Lewy (CFL) number set equal to 1 and resulted in a mean timestep of 0.1 ms. Three complete cardiac cycles were solved and only the third one was used for the post-processing of results to avoid start-up transients.

Regarding the morphological analysis, cross-sectional areas (CSAs) along the models' centerline were taken at 0.1 mm intervals at each timestep to characterize vascular lumen remodeling. Moreover, the evolution during time of the anastomotic angle between the PA and the vein was quantified.

Time changes of blood velocity were characterized using the blood velocity waveforms extracted at nine points sampled consistently along model centerline, at all timepoints after surgery. Moreover, the mean turbulent kinetic energy (TKE) was calculated as

$$TKE = \frac{1}{2} \rho \left(\underline{u'^2} + \underline{v'^2} + \underline{w'^2} \right)$$

where ρ is the blood density and u', v', w' are the fluctuating components of the velocity.[20] The near-wall hemodynamics was investigated using the well-established Oscillatory Shear Index (OSI), that quantifies the degree of variation of the WSS (τ_ω) from its average direction, as

$$OSI = \frac{1}{2} \left(1 - \frac{\left| \int_0^T \tau_\omega dt \right|}{\int_0^T |\tau_\omega| dt} \right)$$

Also, the recently introduced Spectral Power Index (SPI)[21] was computed for the WSS as

$$SPI = \frac{\sum_{n=n_c}^{+\infty} \left| Y[n\omega_0] \right|^2}{\sum_{n=1}^{+\infty} \left| Y[n\omega_0] \right|^2}$$

where $\left| Y[n\omega_0] \right|$ is the magnitude of the Fourier-transformed signal of the WSS, ω_0 is the fundamental angular frequency of the periodic signal, and n_C is the harmonic corresponding to the cut-off frequency set to 25 Hz.

Results

The 3D patient specific AVF models and measured blood flow rates at different time points are reported in Figure 1. Initially, a constant increase of the PA blood flow rate was measured, whose 3 days value has doubled at 40 days, and tripled at 6 months after surgery, an indication of successful maturation in the AVF. At 1 year after surgery the blood flow rate significantly decreased and at 1.5 years it returned to the pre-maturation value, becoming inadequate to perform an efficient HD treatment and resulting in the need of a new VA for the patient. As for qualitative morphological changes, the vessel's lumen dilated at the anastomosis and along the vein during the first 6 months after surgery, then an evident stenosis developed at the curvature of the JAV starting from 1 year after surgery. Moreover, the angle between the PA and the JAV remained unchanged between 3 days and 40 days, and it decreased at 6 months, when it stabilized around a lower value until the end of the follow-up period.
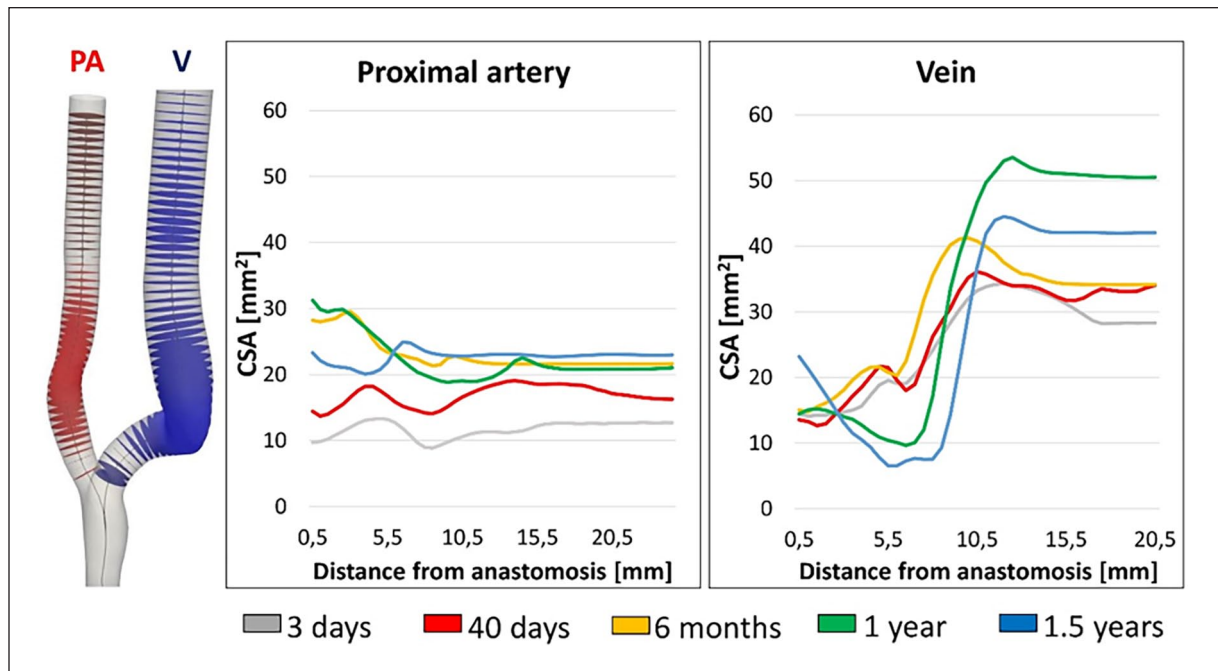
Figure 2. Morphological changes occurring over time in the proximal artery and in the vein.
CSA: cross-sectional area; PA: proximal artery; V: vein.

Local changes in vessel lumen areas are shown in Figure 2. A homogeneous arterial dilatation was observed during VA maturation and up to 6 months (average increase in CSA of +99.7%), with slight regional-specific differences. Later, the PA remained mostly unchanged until 1 year after surgery and decreased at the end of the follow-up period, particularly close to anastomosis. The JAV segment also dilated until 6 months (average increase in CSA of +19.5%). Between 6 months and 1 year the vessel stenosis in the venous segment developed and caused a decrease in CSA of 62.5%, becoming very significant at 1.5 years (−78.8% in CSA).

Velocity–time traces at nine specific points sampled consistently along vessel centerline are shown in Figure 3. Points 1–3 located in the PA, point 4 at the anastomosis, points 5–7 in the JAV, and 8 and 9 more distally in the vein. At all timepoints, velocity traces revealed stable laminar flow in the artery. Immediately after surgery the velocity traces were mostly stable also in the venous segment, with low-amplitude diastolic fluctuations in locations 4–6. Flow instability with high-frequency oscillations developed at 40 days after surgery, when the pulsatile nature of the blood flow waveform was maintained only in points 4 and 5, while it disappeared in points 6–9. At 6 months high-frequency velocity fluctuations were still present, but the pulsatility in the waveform was restored. The fluctuations were found to be damped at 1 year, specifically in the vessel segment where the stenosis developed (points 6 and 7), because of vascular remodeling. The velocity traces then almost completely stabilized along the vein at

1.5 years after surgery, with residual oscillations in the flow waveforms only at the anastomosis (point 4) and in the distal part of the vein (points 8 and 9).

Figure 4 shows the volume rendering of the mean TKE for all timepoints. TKE was negligible in the proximal and distal artery, which is indicative of a laminar flow, at all timepoints after AVF surgery. In contrast, higher TKE values were consistently present at the anastomosis and in the venous segment. Specifically, TKE increased up to 100 J/m^3 within the first 6 months after surgery. Starting from 1 year, TKE values decreased in the venous segment where stenosis developed, but maintaining values up to 30 J/m^3 in the distal segment of the vein.

Surface maps of OSI and SPI are reported in Figure 5. For all timepoints, OSI values are lower than 0.1 in the PA, where the near-wall flow mostly maintains the main direction during the entire cardiac cycle. Areas of high OSI developed in the JAV starting from 40 days after the intervention and were mostly located close to the inner curvature of the vein. One year after surgery, OSI values lower than 0.1 were restored in the first segment of the JAV and in the stenotic area, while areas of high OSI appeared in the distal segment of the vein. Similarly, SPI shows values close to zero in the PA for all timepoints. SPI values increase significantly at the anastomosis and in the venous segment up to 6 months after surgery. At 1 year, null SPI values are restored along the vein as a result of vessel inward remodeling caused by stenosis development. In the distal segment of the vein, the flow instability was still present at 1.5 years after surgery.
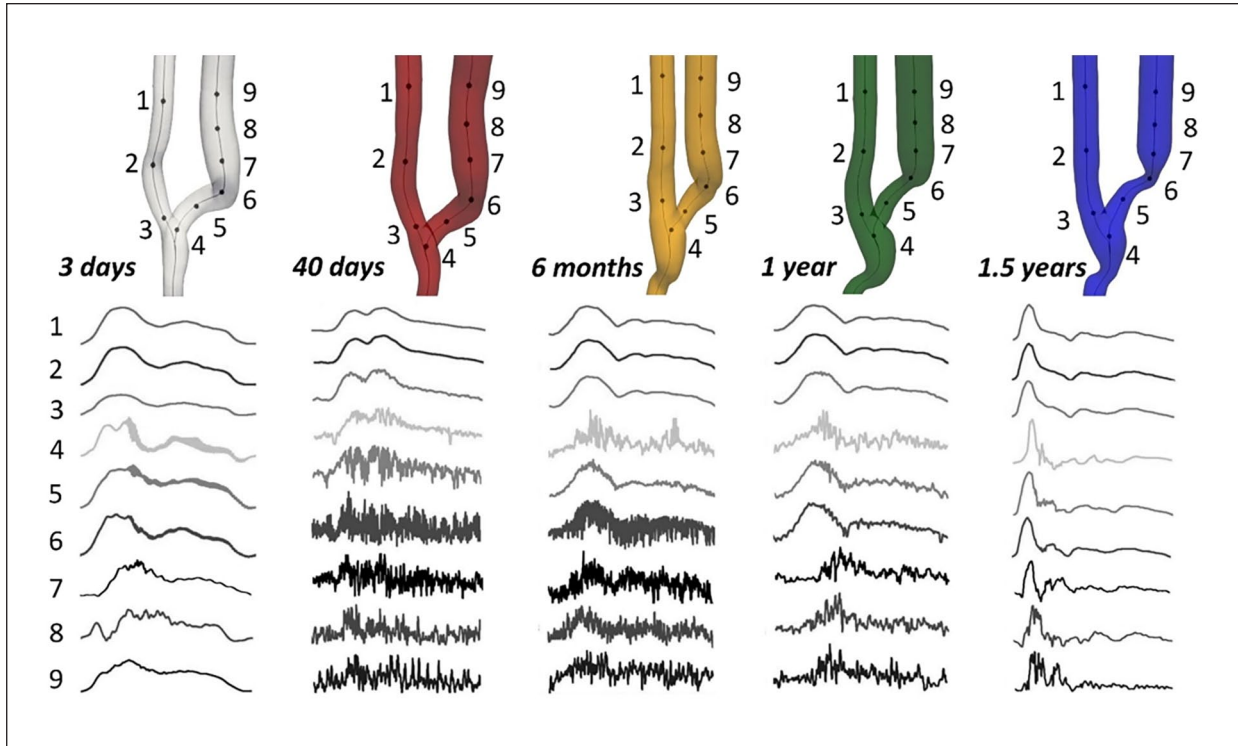
Figure 3. Velocity-time traces, normalized by their respective cycle averages, at nine selected feature points along the centerline of the AVF model corresponding to the five different timepoints.

Figure 4. Volume rendering of the mean turbulent kinetic energy (TKE) at the five different timepoints.
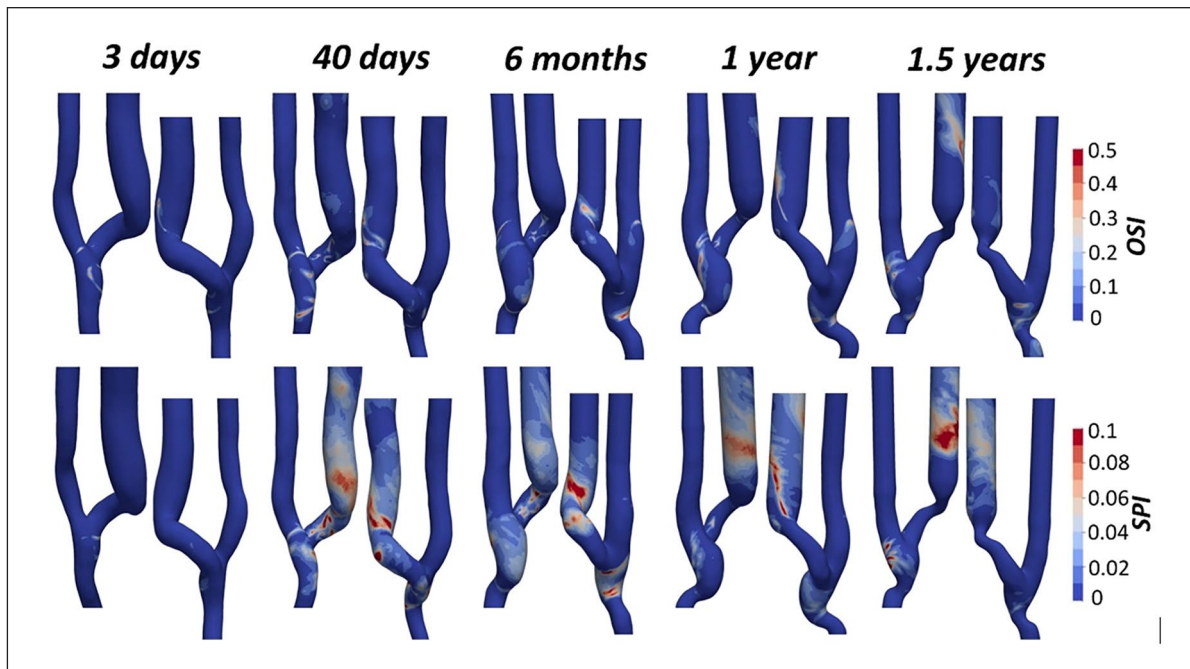
Figure 5. Plot of the Oscillatory Shear Index (OSI) and Spectral Power Index (SPI) surface maps at the five different timepoints.

Discussion

This study assessed the morphological and hemodynamic changes occurring in an AVF over 1.5 years after surgery by five observations during this time interval. The results obtained show that the development of a significant stenosis in the venous segment was paralleled by blood flow velocity stabilization in that region. Specifically, the progressive expansion of the stenotic region over time, as a result of inward remodeling of venous outflow, was accompanied by the regularization of blood flow velocity waveforms in that region and consequent decrease of the near-wall disturbed flow and shear stress metrics.

The longitudinal morphological and hemodynamic characterization of one AVF over five timepoints was an achievement, since only few longitudinal studies to date have focused on AVF remodeling and corresponding changes in the hemodynamics. He et al.[22] and Sigovan et al.[23] have been the first who demonstrated the feasibility of using a contrast-free MRI to CFD pipeline to investigate the morphological and hemodynamic AVF evolution, but no follow-up studies by Sigovan's group trying to relate vascular remodeling to hemodynamic conditions have been published yet. On the contrary, He and collaborators from the HFM Study Group have recently published a large prospective clinical study, with 120 patients and serial assessment of AVF morphology and hemodynamics at 1 day, 6 weeks, and 6 months after surgery. They found that high WSS and low OSI are associated with vessel dilatation,[24] suggesting the potential of conventional hemodynamic parameters for prediction of successful AVF maturation.

Despite the large cohort of patients, and the serial imaging acquisitions and hemodynamic analysis being major strengths of the study, He and coauthors limited their analysis to vessel dilatation or narrowing in the first 6 months after AVF surgery and did not report on the clinical outcome of the AVFs in terms of successful maturation, stenosis development, or excessive vessel dilatation.

To the best of our knowledge, this study is the first that characterized hemodynamic changes occurring during the development of a significant AVF stenosis and its progression to clinical failure, which occurred 1.5 years after surgery. Before stenosis development, the AVF had a successful maturation process, characterized by a massive arterial and venous dilatation within the 6 months after surgery, consistent with the well-established process of AVF maturation. After AVF maturation, the sudden expansion of the venous vessel near the anastomosis was responsible for flow instability and the loss of laminar flow condition, with consequent oscillating wall shear stress. Later, while the arterial diameter stabilized, the JAV started narrowing and caused the AVF failure. These morphological changes were accompanied by an increase in the blood flow rate during the first 6 months, followed by a significant decrease starting from 1 year after surgery, finally returning to the pre-maturation value. More interestingly, we showed that the focal remodeling process in the vein was paralleled by the progressive regularization of blood flow and decrease of near-wall disturbed flow indices in the stenotic area, and a gradual shifting of the unsteady flow patterns along the distal vein. Specifically, the gradual reduction of the vessel cross sectional areas after the anastomosis, in the first

venous segment, reduced progressively the flow instabilities. This process proceeded with time until complete regularization of the flow field in the same venous segment. This evidence suggests that vascular wall remodeling, and more specifically stenosis development, could be the result of a protective mechanism aimed at restoring laminar flow in the AVF, that was turbulent-like after AVF maturation. These results are in line with previous observations showing that the vessels remodel to restore the initial hemodynamic conditions and wall shear stress dynamics.[25]

In our case, vessel remodeling, likely due to intimal hyperplasia, could have been triggered by the presence of flow instability in the AVF vein after maturation and this suggests the presence of a biomechanical stimulus acting on vascular cells. This concept is not new and previous experimental studies have demonstrated that ECs exposed to unidirectional and relatively high WSS display a quiescent phenotype,[26,27] while oscillating flow adjacent to the vessel wall, present in areas of bifurcations or branching, has been suggested to induce a proliferative, pro-inflammatory, pro-oxidant ECs state and an impaired vascular tone regulation.[14,26] Moreover, it has been documented that signals released by ECs induce changes in the underlying vascular SMCs within the vascular wall that cause matrix degradation, cell proliferation and migration that are responsible for vascular wall remodeling.[27] Therefore, the biomechanical stimulus might act at the level of endothelium and then involve SMCs, but a clear explanation of the inward remodeling process has still to be provided. Our results document the dynamics of the inward vessel wall remodeling and its temporal relation to the flow instabilities acting on the vessel wall, induced by massive flow rate increase after surgery. Vessel's inward remodeling progressed until the decrease of vessel diameter caused a reduction of flow instabilities, that progressively damped down, and laminar flow was almost completely restored. It is tempting to speculate that vessel stenosis developed precisely in selected locations of the venous vascular wall as a response of the system to reverse the non-physiological flow instabilities and the fast changes of wall shear stress in time and direction.

From a clinical perspective, this study also raises the question of whether a close surveillance of the AVF hemodynamics may allow to identify AVFs which will develop stenosis. Despite the benefits of AVF surveillance are still debated,[28,29] the US examinations of this patient clearly showed a sudden decrease of blood flow volume and venous diameter between 6 months and 1 year after surgery. Therefore, at 1 year after surgery the narrowing of the vascular lumen and reduction of blood flow rate could have given a precise suggestion to the nephrologist on the need of a timely intervention to prolong AVF patency.

Moreover, highly disturbed hemodynamics at 6 months after surgery could have predicted AVF adverse remodeling. From a clinical perspective, our results suggest that different anastomotic configurations and anastomotic lengths may allow reducing flow instabilities and inducing more helicoidal flow, but additional studies are needed to elucidate the time evolution of the effects of different flow conditions on AVF maturation and long-term patency.

We must acknowledge that the main limitation of the present study is that it includes only one patient. However, the patient under study represented a typical case of radiocephalic AVF and the clinical evolution of his VA was extremely interesting to study stenosis development and progression. Moreover, the US examinations were performed by an experienced clinician, the MR image resolution was previously shown to be adequate for accurate AVF imaging[17] and the hemodynamic analysis were performed with a high temporal and spatial resolution ensuring the accuracy of the simulation results, as reported in previous studies with a number of patients studied at single time point[16] and at three timepoints after AVF creation.[18] Further clinical investigations with a higher number of patients are required to confirm and extend current preliminary findings.

In conclusion, this is the first study that reports a comprehensive analysis of morphological and hemodynamic changes in one AVF failed due to stenosis, over five timepoints, while almost all data previously reported in literature were based on a flow dynamics analysis of a single observation in time, claiming to show the relation between local flow conditions and the effects on vascular remodeling. Our study is the first that can relate the evolution of the local flow conditions and vascular remodeling, showing that the flow instabilities induced after AVF surgery and maturation are responsible for subsequent vessel wall stenosis, with flow regularization and stabilization of unidirectional shear stress, suggesting preliminary evidence of a protective mechanism likely mediated by endothelial cells exposed to fast oscillating wall shear stress. Future longitudinal clinical studies will be needed to provide additional evidence on the role of disturbed flow in stenosis formation, with the final goal of improving AVF clinical outcome.

Acknowledgements

Declaration of conflicting interests

Funding

ORCID iDs

Luca Soliveri 🔗 https://orcid.org/0000-0002-8096-2925

Michela Bozzetto 🔗 https://orcid.org/0000-0002-2045-5550

References

1. Drew DA, Lok CE, Cohen JT, et al. Vascular access choice in incident hemodialysis patients: a decision analysis. *J Am Soc Nephrol* 2015; 26: 183–191.

2. Caroli A, Manini S, Antiga L, et al. Validation of a patient-specific hemodynamic computational model for surgical planning of vascular access in hemodialysis patients. *Kidney Int* 2013; 84(6): 1237–1245.

3. Al-Jaishi AA, Oliver MJ, Thomas SM, et al. Patency rates of the arteriovenous fistula for hemodialysis: a systematic review and meta-analysis. *Am J Kidney Dis* 2014; 63(3): 464–478.

4. Huber TS, Berceli SA, Scali ST, et al. Arteriovenous fistula maturation, functional patency, and intervention rates. *JAMA Surg* 2021; 156(12): 1111.

5. Roy-Chaudhury P, Spergel LM, Besarab A, et al. Biology of arteriovenous fistula failure. *J Nephrol* 2007; 20: 150–163.

6. Lee T and Misra S. New insights into dialysis vascular access: molecular targets in arteriovenous fistula and arteriovenous graft failure and their potential to improve vascular access outcomes. *Clin J Am Soc Nephrol* 2016; 11(8): 1504–1512.

7. Sabiu G and Gallieni M. Pathophysiology of arteriovenous fistula maturation and nonmaturation. *Clin J Am Soc Nephrol* 2023; 18(1): 8–10.

8. Viecelli AK, Mori TA, Roy-Chaudhury P, et al. The pathogenesis of hemodialysis vascular access failure and systemic therapies for its prevention: optimism unfulfilled. *Semin Dial* 2018; 31(3): 244–257.

9. Sivanesan S. Sites of stenosis in AV fistulae for haemodialysis access. *Nephrol Dial Transplant* 1999; 14(1): 118–120.

10. Malek AM. Hemodynamic shear stress and its role in atherosclerosis. *JAMA* 1999; 282(21): 2035.

11. Browne LD, Bashar K, Griffin P, et al. The role of shear stress in arteriovenous fistula maturation and failure: a systematic review. *PLoS ONE* 2015; 10(12): e0145795.

12. Ene-Iordache B and Remuzzi A. Disturbed flow in radial-cephalic arteriovenous fistulae for haemodialysis: low and oscillating shear stress locates the sites of stenosis. *Nephrol Dial Transplant* 2012; 27(1): 358–368.

13. Browne LD, Walsh MT and Griffin P. Experimental and numerical analysis of the bulk flow parameters within an arteriovenous fistula. *Cardiovasc Eng Technol* 2015; 6(4): 450–462.

14. Remuzzi A and Ene-Iordache B. Novel paradigms for dialysis vascular access: upstream hemodynamics and vascular remodeling in dialysis access stenosis. *Clin J Am Soc Nephrol* 2013; 8(12): 2186–2193.

15. Colley E, Simmons A, Varcoe R, et al. Arteriovenous fistula maturation and the influence of fluid dynamics. *Proc Inst Mech Eng* 2020; 234(11): 1197–1208.

16. Bozzetto M, Ene-Iordache B and Remuzzi A. Transitional flow in the venous side of patient-specific arteriovenous fistulae for hemodialysis. *Ann Biomed Eng* 2016; 44(8): 2388–2401.

17. Bozzetto M, Brambilla P, Rota S, et al. Toward longitudinal studies of hemodynamically induced vessel wall remodeling. *Int J Artif Organs* 2018; 41(11): 714–722.

18. Bozzetto M, Soliveri L, Poloni S, et al. Arteriovenous fistula creation with VasQ™ device: a feasibility study to reveal hemodynamic implications. *J Vasc Access*. Epub ahead of print 22 April 2022. DOI: 10.1177/11297298221087160.

19. Antiga L, Piccinelli M, Botti L, et al. An image-based modeling framework for patient-specific computational hemodynamics. *Med Biol Eng Comput* 2008; 46(11): 1097.

20. Les AS, Shadden SC, Figueroa CA, et al. Quantification of hemodynamics in abdominal aortic aneurysms during rest and exercise using magnetic resonance imaging and computational fluid dynamics. *Ann Biomed Eng* 2010; 38(4): 1288–1313.

21. Khan MO, Chnafa C, Gallo D, et al. On the quantification and visualization of transient periodic instabilities in pulsatile flows. *J Biomech* 2017; 52: 179–182.

22. He Y, Terry CM, Nguyen C, et al. Serial analysis of lumen geometry and hemodynamics in human arteriovenous fistula for hemodialysis using magnetic resonance imaging and computational fluid dynamics. *J Biomech* 2013; 46(1): 165–169.

23. Sigovan M, Rayz V, Gasper W, et al. Vascular remodeling in autogenous arterio-venous fistulas by MRI and CFD. *Ann Biomed Eng* 2013; 41(4): 657–668.

24. He Y, Shiu YT, Imrey PB, et al. Association of shear stress with subsequent lumen remodeling in hemodialysis arteriovenous fistulas. *Clin J Am Soc Nephrol* 2023; 18: 72–83.

25. Ene-Iordache B, Mosconi L, Antiga L, et al. Radial artery remodeling in response to shear stress increase within arteriovenous fistula for hemodialysis access. *Endothelium* 2003; 10(2): 95–102.

26. Brahmbhatt A, Remuzzi A, Franzoni M, et al. The molecular mechanisms of hemodialysis vascular access failure. *Kidney Int* 2016; 89(2): 303–316.

27. Franzoni M, Cattaneo I, Longaretti L, et al. Endothelial cell activation by hemodynamic shear stress derived from arteriovenous fistula for hemodialysis access. *Am J Physiol Heart Circ Physiol* 2016; 310(1): H49–H59.

28. Moist L and Lok CE. Con: vascular access surveillance in mature fistulas: is it worthwhile? *Nephrol Dial Transplant* 2019; 34(7): 1106–1111.

29. Tessitore N and Poli A. Pro: vascular access surveillance in mature fistulas: is it worthwhile? *Nephrol Dial Transplant* 2019; 34(7): 1102–1106.